

RESEARCH PAPER

Facile Synthesis and Characterization of Highly Luminescent Bi_2WO_6 Nanoparticles for Photonic Application

Mitra Madani¹, Mohammad Mansourian², Sanaz Almadari^{3,4,*}, Omid Mirzaee^{5,**}, Majid Jafar Tafreshi³

¹ Faculty of Materials Science and Engineering, K.N Toosi University of Technology, Tehran, Iran

² Faculty of Engineering, Payame Noor University, Semnan, Iran

³ Department of Physics, Semnan University, Semnan, Iran

⁴ Applied Science Center, Kharazmi University, Alborz, Iran

⁵ Faculty of Materials and Metallurgical Engineering, Semnan University, Semnan, Iran

ARTICLE INFO

Article History:

Received 19 February 2022

Accepted 26 April 2022

Published 1 May 2022

Keywords:

Optical properties

Luminescence

Synthesize

Bi_2WO_6

ABSTRACT

Facile manufacturing of highly luminescence materials is in demand right now for a wide range of photonic applications. In this work, bismuth tungstate nanoparticles (Bi_2WO_6 NPs) were synthesized using a simple co-precipitation process at room temperature without using any hazardous solvents. The optical and structural properties of the prepared nanopowders were investigated using various techniques, and the photoluminescence measurement was performed using different excitation wavelengths. Bi_2WO_6 NPs were embedded in a flexible matrix, and their photoluminescence property was studied. X-ray diffraction (XRD) and Fourier-transform infrared spectroscopy (FTIR) investigations confirmed the successful synthesis of the related chemical binding in the synthesized nanostructure. According to the FESEM image, cubic-like and spherical-like particles were observed in the average diameter size of 0.9 μm . Some aggregates were detected in the prepared Bi_2WO_6 nanopowder, attributed to the larger Bi_2WO_6 particles. Intense luminescence colors of violet, blue, yellow, and red under ultraviolet excitation were obtained which could be a suitable candidate for photonic application.

How to cite this article

Madani M., Mansourian M., Almadari S., Mirzaee O., Tafreshi M.J. Facile Synthesis and Characterization of Highly Luminescent Bi_2WO_6 Nanoparticles for Photonic Application. *Nanochem Res*, 2022; 7(1):15-21. DOI: 10.22036/ncr.2022.01.003

INTRODUCTION

Semiconductor-based luminescent materials have recently attracted considerable attention due to their advantages in absorbing light for many applications in solving environmental and energy problems [1,2]. For example, long-life, energy-efficient, and environmentally friendly solid-state white lighting equipment based on semiconductor chips and inorganic phosphors has become a popular alternative for ambient lighting. LEDs have already displaced incandescent and fluorescent lights as a new lighting source. A white LED can

be made in several ways. Using red, green, and blue phosphors with UV chips solves the problem of phosphor deterioration and color-changing [3,4]. In addition, using a UV chip with a single-phase phosphor with several emission centers produces a warm-white light. Further, bismuth tungstate (Bi_2WO_6) is considered as a superior matrix material of the tungstate family for photoluminescence materials due to the charge transfer from oxygen to the tungsten under UV light [5-7]. In a recent study, porous metal-organic frameworks were modified by Bi_2WO_6 nanosheets using a facile hydrothermal method for fabricating a photocatalyst with direct Z-scheme heterojunction [8]. In another study,

* Corresponding Author Email: s.alamdari@semnan.ac.ir
o_mirzaee@semnan.ac.ir

the high mineralization efficiency and excellent durability of the Bi_2WO_6 catalyst were demonstrated to remove organic dyes [9]. Generally, few reports have investigated photosensitivity and luminescent properties of Bi_2WO_6 NPs. This paper reports a facile synthesis of Bi_2WO_6 nanopowders via a simple method. The structural, morphological, and optical properties of the synthetic samples were investigated, and the luminescence mechanism of NPs was discussed.

EXPERIMENTAL WORKS AND CHARACTERIZATION

Raw materials and utilized reagents were analytical grades without additional purification. Proper amounts of $\text{Na}_2\text{WO}_4 \cdot 2\text{H}_2\text{O}$ and $\text{Bi}(\text{NO}_3)_3 \cdot 5\text{H}_2\text{O}$ were dissolved in 25 mL distilled water to make solutions A and B, respectively. After 15 min, solution A was progressively added to solution B dropwise under continual magnetic stirring, and instantly a milk-white suspension was generated. The precipitate was collected and washed several times with distilled water and absolute ethanol, and then dried for 24 h. Finally, powders were calcined at 600°C for 2 h to obtain Bi_2WO_6 nanoparticles. A schematic representation of the experimental work is shown in Fig. 1. The phase purity of the as-prepared Bi_2WO_6 particles was examined using X-ray powder diffraction (XRD) with $\text{Cu K}\alpha$ radiation. The particle morphology was investigated by field-

emission scanning electron microscope (FESEM Mira3 TESCAN). FT-IR was performed in the range of $400\text{--}4000\text{ cm}^{-1}$ for studying the functional groups, and photoluminescence (PL) spectroscopy was used to examine the optical characteristics of the produced nanopowders (Cary fluorescence spectrophotometer with $\lambda_{\text{ex}} = 250, 290 \text{ \& } 410\text{ nm}$ at room temperature which featured a xenon lamp, producing 80 powerful flashes per second).

RESULTS AND DISCUSSION

Fig. 2a. shows the XRD patterns of synthesized Bi_2WO_6 NPs in which the diffraction peaks of Bi_2WO_6 particles can be indexed in terms of the tetragonal Bi_2WO_6 phase (PDF card number 96-200-3106). It seems the sample is not sufficiently pure since there are some unknown peaks without Miller indices. This can be solved by increasing the temperature of the calcination and more rinsing (Fig. 2b). The calculated crystallite size of the nanopowders according to the Debye-Scherrer equation was 32 nm. Using equation (1), the crystallite size was calculated from the full width at half maximum (FWHM) of the preferred crystalline plane of the peak [10]:

$$D = \frac{k\lambda}{\beta \cos \theta} \quad (1)$$

Where D is the crystallite size; k refers to the shape factor; λ is the wavelength of the X-ray beams ($\lambda = 1.5406\text{ nm}$ for $\text{Cu K}\alpha$); β is the

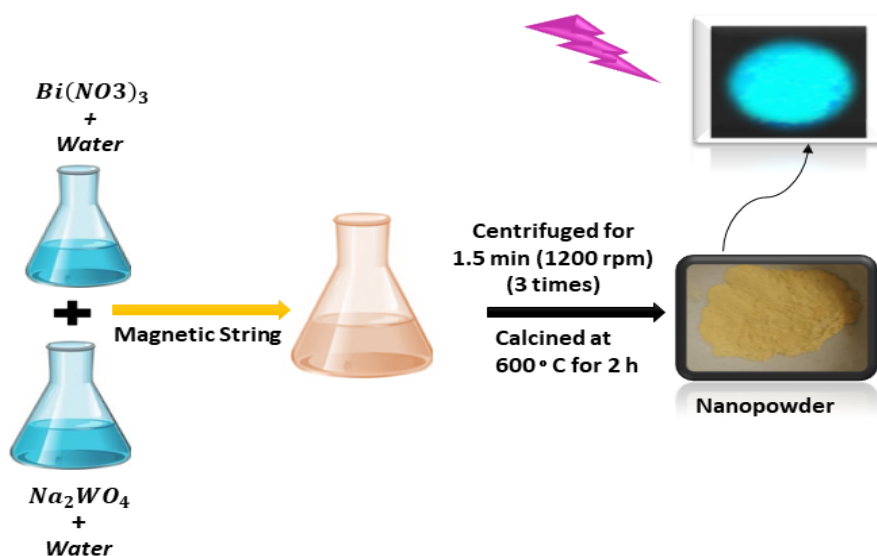


Fig. 1. Brief diagram of experimental works for preparation of sample

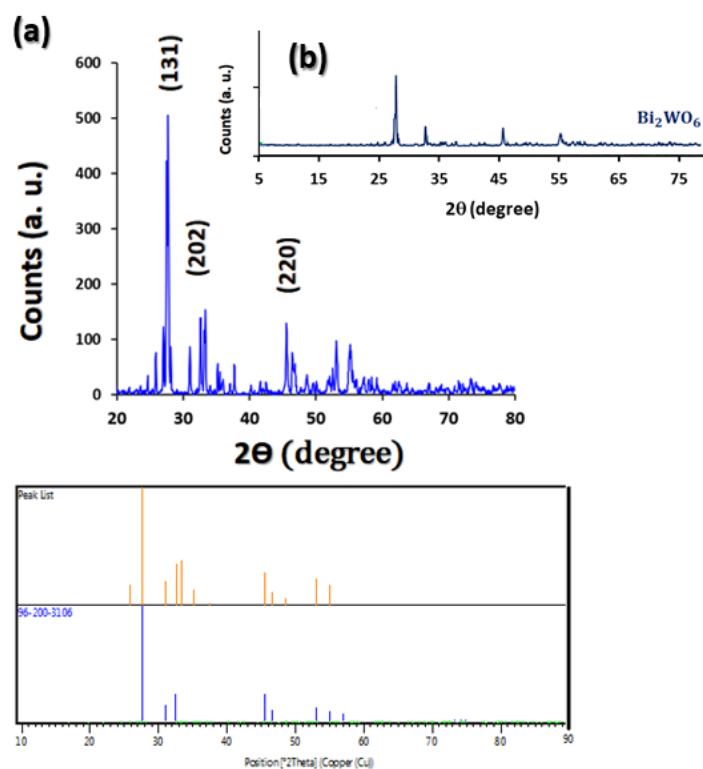


Fig. 2 (a,b). XRD patterns of Bi₂WO₆ NPs.

Table 1. XRD parameters of the synthesized sample

Sample	a (Å)	c (Å)	b (Å)	α (deg)	β (deg)	γ (deg)	Volume of cell (Å ³)
Bi ₂ WO ₆	5.70	17.32	5.71	90.0000	90.0000	90.0000	487

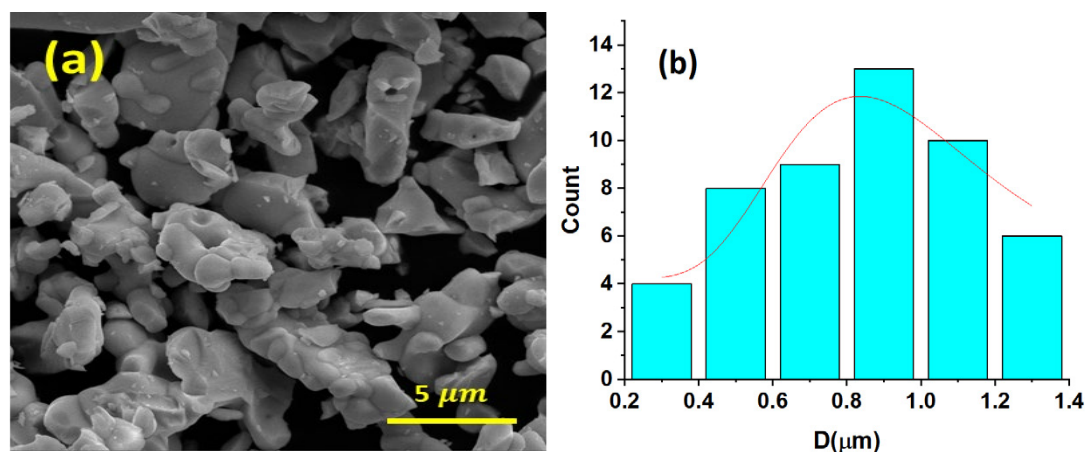
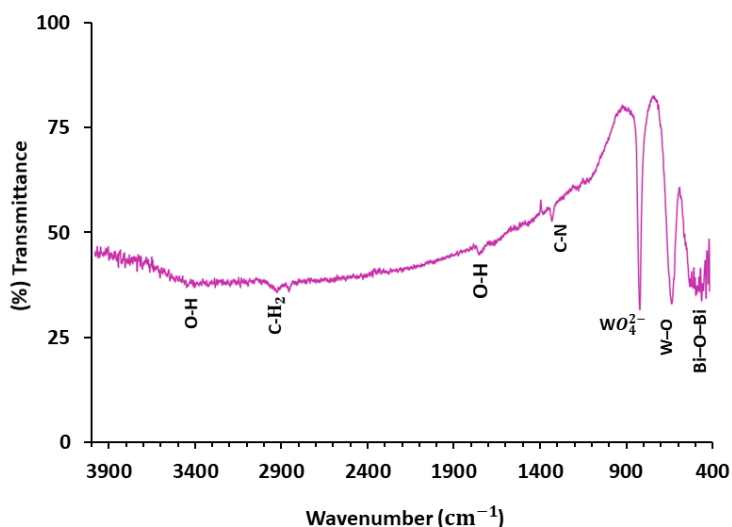
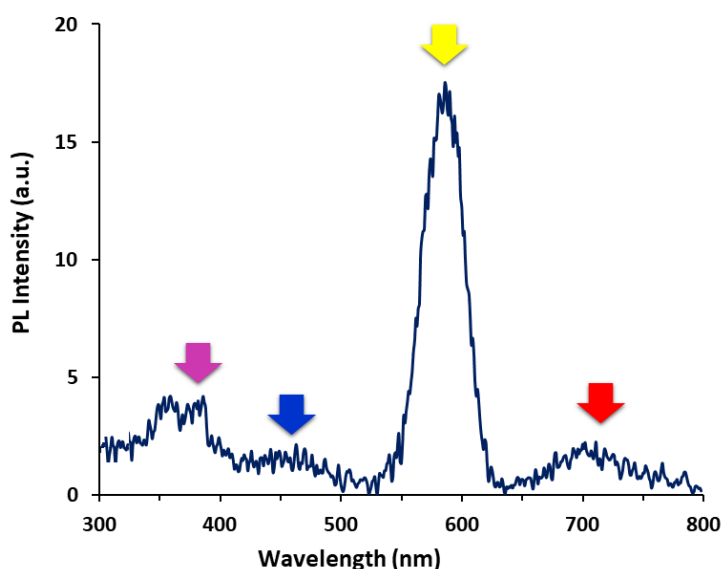


Fig. 3. FEEM image, and (b) size distribution of Bi₂WO₆ NPs

FWHM, and θ is the peak point in radians. It should be noted that this calculation is only a relative estimate of the size along one determined

crystallographic direction, and that the values obtained using the Scherrer formula are not absolute at all. The Scherrer formula was used

Fig. 4. FT-IR spectrum of Bi_2WO_6 sampleFig. 5. Photoluminescence spectrum of synthesized NPs with ≈ 290 nm at room temperature

to estimate the preferred crystalline plane. In addition, the XRD parameters and lattice constants of the synthesized nanopowder were calculated and shown in Table 1.

The morphology and structure were investigated by FESEM (Fig. 3). Cubic-like and spherical-like particles were observed in the average diameter size of $0.92 \mu\text{m}$. Some aggregates were detected in the prepared Bi_2WO_6 nanopowder, attributed to the larger particles.

The FT-IR spectrum of the Bi_2WO_6 NPs is shown in Fig. 4. The bands at 1700 and 3500 cm^{-1} relate to OH stretching, and the peaks at 550 and 750 cm^{-1} correspond to the Bi–O–Bi W–O asymmetric stretches. The in-plane deformation of the WO_4^{2-} group is responsible for the bands at 660 cm^{-1} [10].

PL analysis is usually used for examining photonic carriers' migration, transfer, and separation. The PL spectrum of Bi_2WO_6 NPs

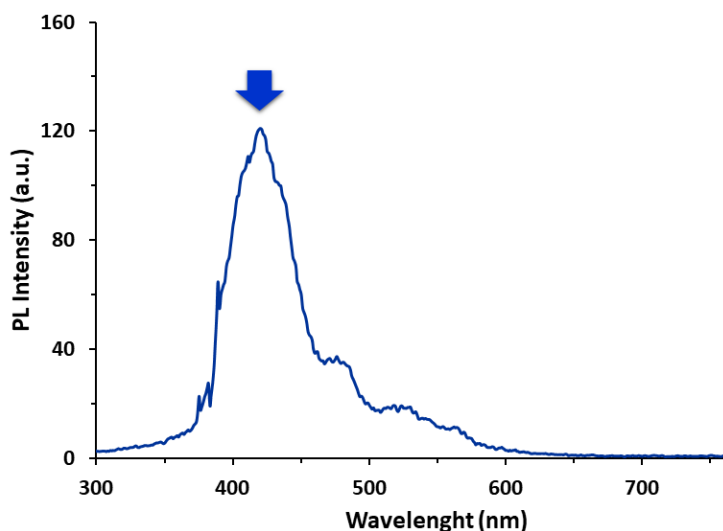


Fig. 6. Photoluminescence spectrum of synthesized NPs with =410 nm at room temperature

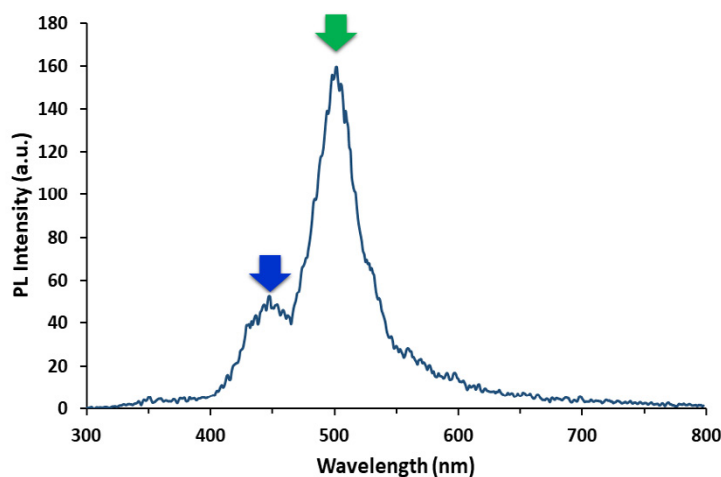


Fig. 7. Photoluminescence spectrum of synthesized NPs with =250 nm at room temperature

is shown in Fig. 5. As is observed with 290 nm UV excitation, three weak violets, blue, and red emission peaks as well as strong yellow emission peaks are obtained in the visible region of wavelengths. The $1A^1-3T^1$ transitions inside the WO_6 complex is responsible for blue-green emission in the WO_4 structure [11,12]. The yellow emission in the spectrum suggests the energy transfer from the WO_6 group to lattice ions [12]. The photoluminescence measurement was conducted at room temperature using different excitation wavelengths. The obtained results are shown in Fig. 6 according to which with an increase in the excitation wavelength (410 nm),

the position of the PL peaks is blue-shifted, and strong blue-green emission was obtained. Further, based on Fig. 7, under an excitation wavelength of 250 nm, strong green emission appeared in the PL spectrum of synthesized nanopowders. Excitation wavelength dependence can arise when the distribution of the molecules in the ground state differ in their solvation sites and energies [13-15]. As a result, tunable emission colors under different excitation wavelengths were obtained at room temperature [17].

Synthesized nanoparticles (0.5 wt.%) were imbedded in polyvinyl alcohol (PVA) matrix by direct mixing method for preparing flexible

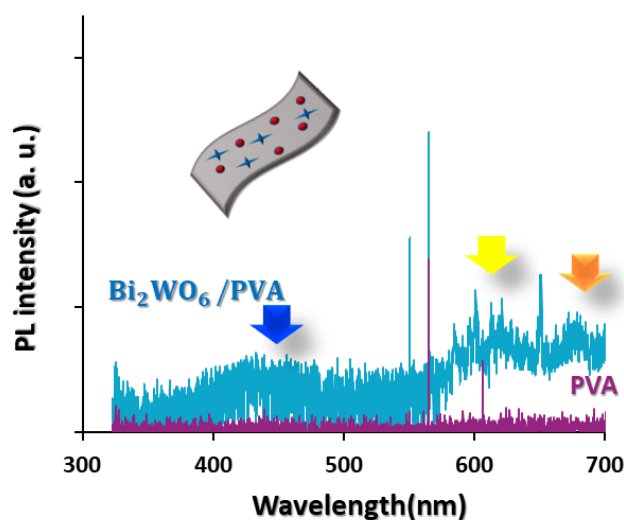


Fig. 8. Photoluminescence spectrum of the prepared flexible $\text{Bi}_2\text{WO}_6/\text{PVA}$ composite film with $\lambda = 290$ nm at room temperature

nanocomposite film, and their PL properties were investigated at room temperature. Luminescence spectrum of the pure PVA and prepared nanocomposite together with an inset schematic image of the prepared sample are shown in Fig. 8. The prepared nanocomposite exhibits strong luminescence peaks while the spectrum of PVA does not show any specific characteristic emission peaks. Based on Fig. 8, flexible $\text{Bi}_2\text{WO}_6/\text{PVA}$ composite film exhibited blue, yellow, and orange emission colors compared with PVA. Therefore, prepared nanocomposite can be a proper candidate for optoelectronic devices applications. In addition, PVA is excited by absorbing light and produces an oscillating dipole, which de-excites the ground state by transferring energy to Bi_2WO_6 non-radiatively. This nonradiative energy stimulates many electrons in the nanocomposite's valence band to the conduction band [17]. Furthermore, the emission state of Bi_2WO_6 releases the majority of the electrons' energy. The augmentation of emission results from nonradiative energy transfer from matrix to Bi_2WO_6 . Shallow levels as an activator ion introduce extra ground-state and excited-state levels of energies between the valence and conduction bands of the Bi_2WO_6 nanocomposite. An electron with sufficiently high excitation energy is elevated to the conduction band, travels away from the center, and may be trapped by a lattice defect or return to an ionized center. There it initially occupies an exciting level and then emits a photon to return to the ground state of the activator center [15,17]. Generally, few reports have investigated photosensitivity and luminescent

properties of Bi_2WO_6 NPs. This research reports a facile synthesis of highly luminescent Bi_2WO_6 nanopowders via a simple method.

CONCLUSION

Bi_2WO_6 nanoparticles with an average size of $\sim 0.9 \mu\text{m}$ were successfully prepared via a simple route. The facile synthesized nanopowders exhibited visible emission colors under UV excitation at room temperature. In fact, tunable emission colors under different excitation wavelengths were obtained at room temperature which can be considered as a good candidate for future white emitting diode applications.

ACKNOWLEDGMENTS

The authors would like to acknowledge the Iranian National Elites Foundation for the financial support of this research.

COMPLIANCE WITH ETHICAL STANDARDS

All the authors declare that they have no conflict of interest.

REFERENCES

- [1] Huang C-S, Jakubowski K, Ulrich S, Yakunin S, Clerc M, Toncelelli C, et al. Nano-domains assisted energy transfer in amphiphilic polymer conetworks for wearable luminescent solar concentrators. *Nano Energy*. 2020;76:105039.
- [2] Fang W, Zhao H, Jia T, Fu Q, Xu C, Tao H, et al. Effects of La and Ni doping on ferroelectric and photocatalytic properties of Aurivillius $\text{Bi}_7\text{T}_3\text{Fe}_3\text{O}_{21}$. *Solid-State Electronics*. 2021;186:108170.
- [3] Xia Z, Liu Q. Progress in discovery and structural design of

- color conversion phosphors for LEDs. *Progress in Materials Science*. 2016;84:59-117.
- [4] Bi Z, Jia K, Liu Y, Lyu Y. Tunable Luminescence Properties and Elucidating the Electronic Structures of Single-Phase Spherical BaWO₄: Dy³⁺, Tm³⁺, Eu³⁺ Phosphors for Warm-White-Lighting. *Journal of Renewable Materials*. 2022;10(2):431.
- [5] Newkirk HW, Quadflieg P, Liebertz J, Kockel A. Growth, crystallography and dielectric properties of Bi₂WO₆. *Ferroelectrics*. 1972;4(1):51-5.
- [6] Utkin V, Roginskaya YE, Voronkova V, Yanovskii V, Sh. Galyamov B, Venetsev YN. Dielectric properties, electrical conductivity, and relaxation phenomena in ferroelectric Bi₂WO₆. *physica status solidi (a)*. 1980;59(1):75-82.
- [7] Wang D, Xue G, Zhen Y, Fu F, Li D. Monodispersed Ag nanoparticles loaded on the surface of spherical Bi₂WO₆ nanoarchitectures with enhanced photocatalytic activities. *Journal of Materials Chemistry*. 2012;22(11):4751-8.
- [8] He Y, Wang D, Li X, Fu Q, Yin L, Yang Q, et al. Photocatalytic degradation of tetracycline by metal-organic frameworks modified with Bi₂WO₆ nanosheet under direct sunlight. *Chemosphere*. 2021;284:131386.
- [9] Lei H, Wu M, Liu Y, Mo F, Chen J, Ji S, et al. Built-in piezoelectric field improved photocatalytic performance of nanoflower-like Bi₂WO₆ using low-power white LEDs. *Chinese Chemical Letters*. 2021;32(7):2317-21.
- [10] Wang S, Yang H, Yi Z, Wang X. Enhanced photocatalytic performance by hybridization of Bi₂WO₆ nanoparticles with honeycomb-like porous carbon skeleton. *Journal of Environmental Management*. 2019;248:109341.
- [11] Wang J, Zhang Z-J, Zhao J-T, Chen H-H, Yang X-X, Tao Y, et al. Luminescent metastable Y₂WO₆:Ln³⁺ (Ln = Eu, Er, Sm, and Dy) microspheres with controllable morphology via self-assembly. *Journal of Materials Chemistry*. 2010;20(48):10894-900.
- [12] Tian L, Yang P, Wu H, Li F. Luminescence properties of Y₂WO₆:Eu³⁺ incorporated with Mo⁶⁺ or Bi³⁺ ions as red phosphors for light-emitting diode applications. *Journal of Luminescence*. 2010;130(4):717-21.
- [13] Irimpan L, Krishnan B, Deepthy A, Nampoori VPN, Radhakrishnan P. Excitation wavelength dependent fluorescence behaviour of nano colloids of ZnO. *Journal of Physics D: Applied Physics*. 2007;40(18):5670-4.
- [14] Knight KS. The crystal structure of ferroelectric Bi₂WO₆ at 961 K. *Ferroelectrics*. 1993;150(1):319-30.
- [15] Ghamsari MS, Alamdari S, Razzaghi D, Arshadi Pirlar M. ZnO nanocrystals with narrow-band blue emission. *Journal of Luminescence*. 2019;205:508-18.
- [16] Alamdari S, Jafar Tafreshi M, Sasani Ghamsari M, Majles Ara MH. Preparation and Characterization of ZnO and CdWO₄ Nanopowders for Radiation Sensing. *Progress in Physics of Applied Materials*. 2021;1(1):14-8.
- [17] Alamdari S, Majles Ara MH, Jafar Tafreshi M. Synthesize and optical response of ZnO/CdWO₄: Ce nanocomposite with high sensitivity detection of ionizing radiations. *Optics & Laser Technology*. 2022;151:107990.